THE JOURNAL OF BIOLOGICAL CHEMISTRY VOL. 283, NO. 44, pp. 30121–30128, October 31, 2008


# Intramembrane Proteolysis of G*X*GD-type Aspartyl Proteases Is Slowed by a Familial Alzheimer Disease-like Mutation*[S]

Received for publication, August 6, 2008, and in revised form, August 28, 2008 Published, JBC Papers in Press, September 3, 2008, DOI 10.1074/jbc.M806092200

**Regina Fluhrer[‡], Akio Fukumori[‡], Lucas Martin[‡1], Gudula Grammer[‡], Martina Haug-Kröper[‡], Bärbel Klier[‡], Edith Winkler[‡], Elisabeth Kremmer[§], Margaret M. Condron[¶], David B. Teplow[¶], Harald Steiner[‡], and Christian Haass[‡2]**

*From the [‡]Center for Integrated Protein Science Munich and Adolf-Butenandt-Institute, Department of Biochemistry, Laboratory for Neurodegenerative Disease Research, Ludwig-Maximilians-University, Munich 80336, Germany, the [§]Institute of Molecular Immunology, Helmholtz Zentrum München, Marchioninistr. 25, Munich 81377, Germany, and the [¶]Department of Neurology, David Geffen School of Medicine, and Molecular Biology Institute and Brain Research Institute, University of California, Los Angeles, California 90095*

**More than 150 familial Alzheimer disease (FAD)-associated missense mutations in presenilins (PS1 and PS2), the catalytic subunit of the γ-secretase complex, cause aberrant amyloid β-peptide (Aβ) production, by increasing the relative production of the highly amyloidogenic 42-amino acid variant. The molecular mechanism behind this pathological activity is unclear, and different possibilities ranging from a gain of function to a loss of function have been discussed. γ-Secretase, signal peptide peptidase (SPP) and SPP-like proteases (SPPLs) belong to the same family of G*X*GD-type intramembrane cleaving aspartyl proteases and share several functional similarities. We have introduced the FAD-associated PS1 G384A mutation, which occurs within the highly conserved G*X*GD motif of PS1 right next to the catalytically critical aspartate residue, into the corresponding G*X*GD motif of the signal peptide peptidase-like 2b (SPPL2b). Compared with wild-type SPPL2b, mutant SPPL2b slowed intramembrane proteolysis of tumor necrosis factor α and caused a relative increase of longer intracellular cleavage products. Because the N termini of the secreted counterparts remain unchanged, the mutation selectively affects the liberation of the intracellular processing products. *In vitro* experiments demonstrate that the apparent accumulation of longer intracellular cleavage products is the result of slowed sequential intramembrane cleavage. The longer cleavage products are still converted to shorter peptides, however only after prolonged incubation time. This suggests that FAD-associated PS mutation may also result in reduced intramembrane cleavage of β-amyloid precursor protein (βAPP). Indeed, *in vitro* experiments demonstrate slowed intramembrane proteolysis by γ-secretase containing PS1 with the G384A mutation. As compared with wild-type PS1, the mutation selectively slowed Aβ40 production, whereas Aβ42 generation remained unaffected. Thus, the PS1 G384A mutation causes a selective loss of function by slowing the processing pathway leading to the benign Aβ40.**

Research on the proteolytic generation of the Alzheimer's disease (AD)[3]-associated amyloid β-peptide (Aβ) from its precursor, the β-amyloid precursor protein (βAPP) paved the way to the concept of regulated intramembrane proteolysis (1). Already early work suggested that, upon ectodomain shedding of βAPP, the remaining membrane-retained stub, the APP C-terminal fragment undergoes intramembrane proteolysis by a physiologically normal mechanism (2–4) (Fig. 1). Intramembrane proteolysis is now known for many substrates and either required for the generation of a transactivating intracellular domain (ICD) or for a rather general removal of membrane-retained protein stubs (a membrane proteasome function) (5). The intramembrane cleaving protease of βAPP turned out to be a high molecular weight complex, termed γ-secretase, which is composed of four subunits, presenilin (PS1 or PS2), Nicastrin, APH-1a/b, and PEN-2 (6). The four components are required and sufficient for γ-secretase activity (7). PSs share a common active site motif within transmembrane domain (TM) 7, the G*X*GD motif (8, 9). This motif is also present in several other proteases such as the type IV prepilin peptidases, the signal peptide peptidase (SPP), and the SPP-like proteases (SPPL2a, SPPL2b, and SPPL3) (10, 11) and now defines the novel class of G*X*GD-type intramembrane cleaving aspartyl proteases (8). In contrast to γ-secretase, members of the SPP family appear not to require additional components but are rather proteolytically active by themselves (10, 12). In addition, SPP family members exclusively accept transmembrane proteins in a type II orienta-

* This work was supported, in whole or in part, by National Institutes of Health Grant NS038328 (to D. B. T.). This work was also supported by the Leibniz Award of Deutsche Forschungsgemeinschaft (DFG, to C. H.), by the Collaborative Research Center Molecular Mechanisms of Neurodegeneration (Grant SFB 596 to C. H., H. S., and E. K.), by DFG Grant HA1737-11-1 (to C. H. and R. F.), and by the Center for Integrated Protein Science Munich and the Alzheimer Research Award of the Hans and Ilse Breuer Foundation (to H. S.). The costs of publication of this article were defrayed in part by the payment of page charges. This article must therefore be hereby marked "*advertisement*" in accordance with 18 U.S.C. Section 1734 solely to indicate this fact.

[S] The on-line version of this article (available at http://www.jbc.org) contains supplemental Fig. S1.

[1] A member of the ENB (Elitenetzwerk Bayern) Graduate Program "Protein Dynamics in Health and Disease."

[2] Supported by a Research Professorship provided by the LMU[excellent] program. To whom correspondence should be addressed: Tel.: 49-89-2180-75-471; Fax: 49-89-2180-75-415; E-mail: chaass@med.uni-muenchen.de.

[3] The abbreviations used are: AD, Alzheimer disease; ER, endoplasmic reticulum; FAD, familial Alzheimer disease; FL, full length; ICD, intracellular domain; NTF, N-terminal fragment; PS, presenilin; APP, amyloid precursor protein; SPP, signal peptide peptidase; SPPL, signal peptide peptidase-like; TM, transmembrane domain; TNFα, tumor necrosis factor α; $(Z\text{-LL})_2$-ketone, 1,3-di-(*N*-benzyloxycarbonyl-L-leucyl-L-leucyl)amino acetone; wt, wild type; HA, hemagglutinin; Tricine, *N*-[2-hydroxy-1,1-bis(hydroxymethyl)ethyl]glycine.

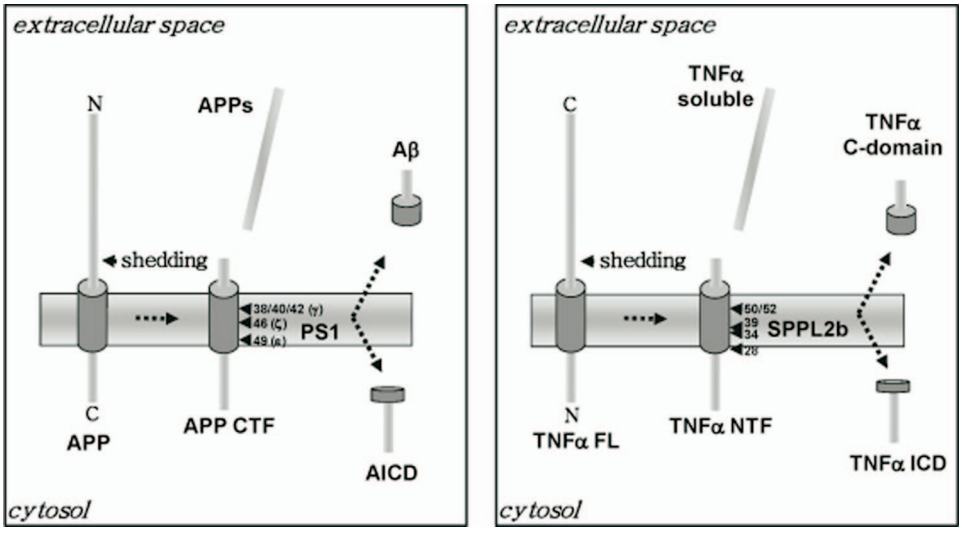


FIGURE 1. **Intramembrane proteolysis of APP *versus* TNFα.** Schematic representation of the proteolytic processing of APP and TNFα by γ-secretase/PS1 and SPPL2b, respectively.

tion as substrates (10, 12–15), whereas for γ-secretase only type-I-oriented substrates have been described so far (Fig. 1) (6). The SPP family members are differentially distributed within the secretory pathway (14, 16), a fact that may reflect their preference for certain substrates located within the respective compartments. Consistent with that hypothesis, SPP is found within the endoplasmic reticulum, where it is involved in the degradation of signal peptides. Besides degradation of signal peptides, SPP is also involved in immune surveillance, intramembrane processing of the hepatitis C virus core protein (10), and dislocation from the endoplasmic reticulum (17). For the Golgi and endosome/lysosome-located SPPL2a and its close homologue SPPL2b, so far three different substrates have been identified, tumor necrosis factor α (TNFα) (12, 14), the Fas-ligand (13), and Bri2 (British dementia protein-2 or Itm2b) (15). Intramembrane proteolysis of TNFα leads to the generation of an ICD, which is required for reverse signaling and regulation of interleukin-12 levels (14). Interestingly, both γ-secretase and SPPL2b substrates undergo multiple and similar intramembrane cleavages (12, 18) (Fig. 1). For γ-secretase it appears that a cleavage oriented more toward the cytoplasm (ϵ-cleavage) leads to the liberation of an ICD (19–21), whereas additional cleavages (ζ- and γ-cleavages) in the middle of the membrane are required to finally release small peptides, including Aβ into the extracellular space (6, 22) (Fig. 1). Because SPP family members cleave type-II proteins (Fig. 1) and their protease active sites are in the opposite orientation as those of PS (23), one may also expect opposite cleavage reactions, a hypothesis that is supported by the results presented in this study.

PSs contain the most frequently observed FAD-associated mutations (6). Until now more than 150 PS mutations have been described, which probably all cause early onset AD by a subtle shift of the γ-cleavage within TM of βAPP from position 40 to position 42 of Aβ. The 42-amino acid Aβ42 is highly prone to aggregation and forms neurotoxic Aβ oligomers, which affect long term potentiation and neuronal survival (24). The exact molecular mechanism behind this shift in cleavage precision is currently unclear. However, evidence exists that PS mutations may affect the proximity of the PS N-terminal and C-terminal fragment within the active γ-secretase complex (25). This may indicate that PS mutations induce structural changes affecting the protease active site embedded within TM6 of the PS NTF and TM7 of the PS C-terminal fragment. Early work already demonstrated that FAD-associated PS mutations fail to rescue the Notch phenotype caused by the loss of the PS homologue in *Caenorhabditis elegans* while wt human PS was fully functional (26, 27). Moreover, several rather aggressive PS mutations have been described, which strongly inhibit the production of the Notch ICD (28). Nevertheless at least some PS mutations appear to rescue the Notch phenotype observed in PS knockout mice (29). Thus, it is unclear if FAD-associated PS mutations cause a loss or a (toxic) gain of function (30–32). Insights into the pathological mechanisms of PS mutations are highly important not only for the understanding of FAD but also for future treatment strategies aiming to inhibit γ-secretase activity. We have now introduced the FAD-associated PS1 G384A mutation (9) into the homologous and highly conserved motif of SPPL2b. Surprisingly, this results in the accumulation of a longer ICD, which was produced by a slowed sequential cleavage within the membrane of the SPPL2b substrate TNFα. Similar findings were made with the PS1 G384A mutation, which in comparison to wt PS1 exhibits a selectively slowed production of Aβ40, whereas the rate of Aβ42 generation is largely unaffected.

## EXPERIMENTAL PROCEDURES

*Cell Culture, cDNAs, and Transfection*—HEK 293 TR cells (Invitrogen GmbH, Karlsruhe, Germany) were cultured in Dulbecco's modified Eagle's medium with Glutamax (Invitrogen) supplemented with 10% fetal calf serum (Invitrogen), 5 μg/ml blasticidin (Invitrogen), and 1% penicillin/streptomycin (Invitrogen). Using PCR, a HA tag (AYPYDVPDYA) and a stop codon were added to the C termini of all constructs. SPPL2b wt, SPPL2b D421A, and SPPL2b G420A were subcloned into the EcoRI and XhoI sites of pcDNA 4/TO/myc/his A (Invitrogen) and stably transfected into HEK 293 TR cells. Transfection of cells was carried out using Lipofectamine 2000 (Invitrogen) according to the manufacturer's instructions, and single cell clones were generated by selection in 200 μg/ml Zeocin (Invitrogen). To induce expression of the SPPL2b constructs, cells were incubated with 1 μg/ml doxycycline (BD Biosciences, San Jose, CA) added to the cell culture medium for at least 48 h. HEK 293 cells stably co-expressing swAPP and PS1 wt or PS1 G384 have been described (28).

The TNFα cDNA was obtained from ATCC (clone AAA61198). Upon addition of a N-terminal FLAG tag (DYKDDDDK) after the starting methionine and a C-terminal HA tag

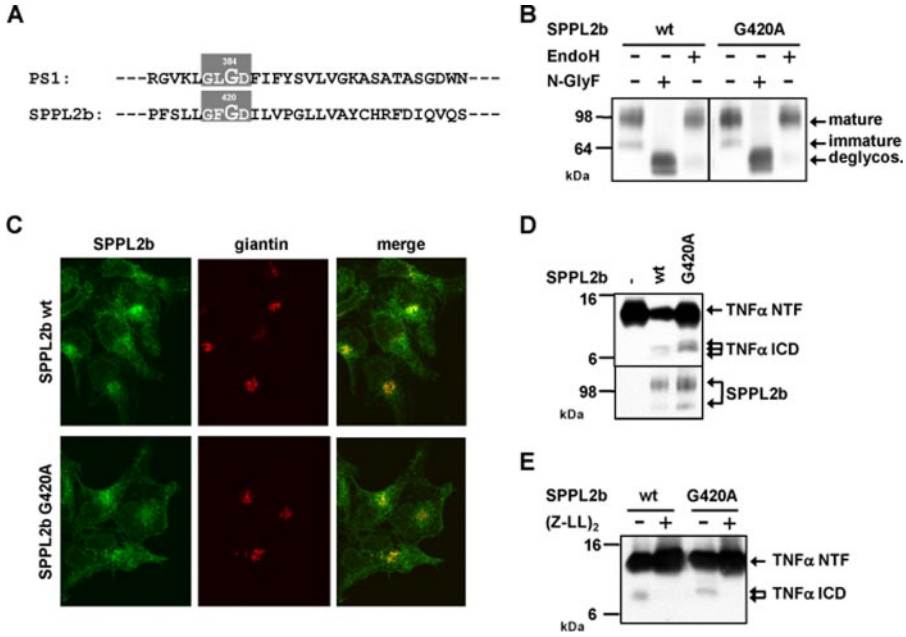


FIGURE 2. **Proteolytic processing of TNFα by SPPL2b.** *A*, amino acid alignment of PS1 and SPPL2b. Amino acids of TM 7 of PS1 and SPPL2b are depicted using the single letter code. The conserved G*X*GD motive in the catalytically active site of PS1 and SPPL2b is highlighted by the *gray box*. The mutagenized glycine residue in PS1 and SPPL26 is shown in *bold*. *B*, post-translational maturation of SPPL2b variants. Protein extracts of HEK 293 cells stably expressing the indicated SPPL2b variants were treated with *N*-glycosidase F (*N-Gly F*) or endoglycosidase H (*EndoH*). SPPL2b variants were detected using the monoclonal anti-HA antibody (Roche Applied Science). Note endoglycosidase H resistance of all SPPL2b variants. *C*, cellular localization of SPPL2b variants. Immunohistochemical staining of SPPL2b wt and SPPL2b G420A using the polyclonal anti HA-antibody. SPPL2b wt and SPPL2b G420A show identical subcellular localization. *D*, TNFα ICD generation. HEK 293 cells stably expressing the indicated SPPL2b variants were transiently transfected with full-length TNFα. Cellular membranes were isolated, incubated for 15 min at 37 °C, and subjected to SDS-PAGE and Western blot analysis. TNFα N-terminal fragments were visualized using the anti-FLAG antibody. Expression levels of SPPL2b variants are shown in the *lower panel*. Note that the TNFα ICD detected in SPPL2b G420A-expressing cells migrates slower than the ICDs detected in SPPL2b wt-expressing cells. *E*, pharmacological inhibition of SPPL2b G420A prevents TNFα ICD generation. Membranes of HEK 293 cells described in *D* were isolated and incubated in the presence of 15 μM $(Z\text{-}LL)_2$-ketone or the respective carrier for 15 min at 37 °C. TNFα N-terminal fragments were detected as described in *D*. Note that $(Z\text{-}LL)_2$-ketone treatment inhibits TNFα ICD generation in SPPL2b wt and in SPPL2b G420A-expressing cells to the same extent.

(YPYDVPDYA) or a C-terminal V5 tag (GKPIPNPLLGLDST) the TNFα cDNA construct was subcloned into the HindIII/XhoI sites of pcDNA 3.1. Hygro+ (Invitrogen). The C-terminally truncated TNFα ΔE construct has been described before (12). TNFα cDNA constructs were co-transfected with the respective SPPL2b variant using Lipofectamine 2000 (Invitrogen Life Sciences) according to the supplier's instructions. All cDNA constructs were sequenced for verification.

*Antibodies, Immunoprecipitation, Immunohistochemical Staining, Immunoblotting, and Deglycosylation Experiments*—The monoclonal anti-HA antibody was obtained from Roche Diagnostics GmbH (Mannheim, Germany). The monoclonal anti-FLAG M2 and the polyclonal HA 6908 antibody were obtained from Sigma. A monoclonal antibody to amino acids 536–557 of SPPL2b was generated (CPSE-1H5). The monoclonal anti Aβ antibody 6E10 was purchased from Signet Laboratories. The polyclonal antibody 6687 to the C terminus of APP has been described (9). To separate individual Aβ species a bis-Tricine-urea gel-system described earlier was used (33). For the separation of TNFα ICD species a modified Tris-Tricine gel was used (12). Immunoprecipitation, deglycosylation, immunohistochemical staining, and immunoblotting experiments were carried out as described previously (12, 16).

*TNFα and C100 in Vitro Processing Assays*—TNFα *in vitro* processing assays were carried out as described before (12). Where indicated, cells were treated with the SPPL2b inhibitor $(Z\text{-}LL)_2$-ketone (Calbiochem) (34) or protease inhibitor mixture (Sigma). Proteins were immunoblotted and detected using the enhanced chemiluminescence technique (GE Healthcare, Little Chalfont, UK). For quantitation the chemiluminescence signals of at least three independent experiments were measured with a CD camera-based imaging system (Alpha Innotec, Kasendorf, Germany). γ-Secretase *in vitro* assays were carried out as described using recombinant $C100\text{-}His_6$ substrate (7). A partially purified γ-secretase preparation was used as enzyme source.[4]

*Radiosequencing*—HEK 293 cells stably expressing SPPL2b wt and transiently expressing TNFαΔE were metabolically labeled with [$^3$H]valine or [$^3$H]leucine (Hartmann Analytic, Germany) for 16 h, supernatants were collected, and TNFα C-domain peptides were isolated by immunoprecipitation with antibody HA6908 (Sigma) separated by SDS-PAGE and transferred to a polyvinylidene difluoride membrane. Radiolabeled proteins were detected by autoradiography, excised, and subjected to radiosequencing, essentially as described (3, 35).

## RESULTS

*Altered Proteolytic Processing of TNFα by SPPL2b Carrying an FAD-like Mutation*—γ-Secretase and SPP/SPPL family members share a number of similar biochemical properties (18, 36). Moreover, several sequence motifs in the catalytic subunits of γ-secretase, PS1 or PS2, and SPP family members are conserved. These include the two active site domains, the YD and G*X*GD motif in TM6 and TM7, as well as a PAL motive in TM9 (10, 11, 16), which likely also contributes to the catalytic site (37). A very aggressive FAD-associated PS1 mutation (PS1 G384A) immediately N-terminal to the critical aspartate residue in TM7 of PS1 helped to elucidate the importance of the G*X*GD domain for PS and led to the definition of the new family of G*X*GD-type aspartyl proteases (8, 9). The PS1 G384A mutation (Fig. 2*A*) strongly affects the precision of the γ-secretase cleavage causing a substantial relative increase of pathological Aβ42 (9, 38). To prove if such a single amino acid exchange

[4] Winkler *et al.*, manuscript in preparation.

could also affect the cleavage precision of other G*X*GD-type aspartyl proteases, the corresponding conserved glycine residue in SPPL2b was mutagenized to alanine, creating SPPL2b G420A (Fig. 2*A*). Like wt SPPL2b, the SPPL2b G420A mutant became endoglycosidase H-resistant upon expression in HEK 293 cells, which is consistent with normal transport through the secretory pathway (Fig. 2*B*). Moreover, mutant and wt SPPL2b showed a similar distribution within the secretory pathway, including a giantin-positive Golgi compartment (Fig. 2*C*). Co-expression of TNF$\alpha$, the only SPPL2b substrate with a known physiological function (14), allows monitoring of intramembrane proteolysis (12). As reported before (12), wt SPPL2b produces ~6-kDa TNF$\alpha$ ICD peptides (Fig. 2*D*). ICD formation also occurs upon expression of the FAD-like SPPL2b G420A mutation (Fig. 2*D*). Interestingly, the ICD peptides produced under these conditions by the SPPL2b G420A mutation migrated at a slightly higher molecular weight (Fig. 2*D*). The elongated TNF$\alpha$ ICD peptide is a specific cleavage product of SPPL2b G420A, because its generation is blocked by $(Z\text{-}LL)_2$-ketone, a selective inhibitor of the SPP-family (Fig. 2*E*) (10). These findings may suggest that the FAD-like mutation exhibits an altered activity, which in analogy to mutant PS may lead to the generation of a slightly elongated cleavage product. However, in clear contrast to the elongated A$\beta$ peptide produced by mutant $\gamma$-secretase, this fragment accumulates within cell lysates. Thus, consistent with the reverse orientation of the active site motifs in TM6 and TM7 (23), the products of intramembrane proteolysis of TNF$\alpha$ by SPPL2b are released into the opposite direction as compared with $\gamma$-secretase substrates.

*Mutant SPPL2b Does Not Affect the Generation of the Secreted TNF$\alpha$ C-domain*—To prove the reverse release of SPPL2b cleavage products as compared with $\gamma$-secretase cleavage products, we next analyzed the secreted TNF$\alpha$ C-domain (Fig. 1). Upon co-expression of the C-terminal HA-tagged TNF$\alpha\Delta$E (12) with either SPPL2b wt or SPPL2b G420A the TNF$\alpha$ C-domain was secreted into the medium like in cells expressing SPPL2b wt (Fig. 3*A*). Interestingly, and in contrast to the ICDs, the TNF$\alpha$ C-domains produced by wt and G420A mutant SPPL2b co-migrated suggesting equal cleavage sites (Fig. 3*A*). To ensure that the C-domain species secreted from the two cell lines are indeed produced by endoproteolytic cleavage at identical sites we radiosequenced their N termini. Sequencing the N termini of the secreted C-domain species from either SPPL2b wt- or SPPL2b G420A-expressing cells revealed no difference in the cleavage site (Fig. 3*B*). Both, mutant and wt SPPL2b produced peptides with N termini starting at leucine 50 or histidine 52. Both C-domain species produced by each cell line (Fig. 3*A*) were radiosequenced and demonstrated to have identical N termini (data not shown). Thus differences in the running behavior are either due to aberrant folding or the lack of a few amino acids on the C termini of the faster migrating species. These findings suggest that an FAD-like mutation in SPPL2b shifts the intramembrane cleavage of its substrate like mutant $\gamma$-secretase. However, consistent with the opposite orientation of the protease active site domains (23) and the type-II orientation of the TNF$\alpha$ substrate, the elongated product was not secreted like A$\beta$42 but released into the cytosol (Fig. 2*D*). Thus, our findings demonstrate that the malfunction of FAD-associated PS mutations can be transferred to other members of the G*X*GD-type proteases. Moreover, our findings provide direct evidence for a reversed orientation/activity of SPPL2b.

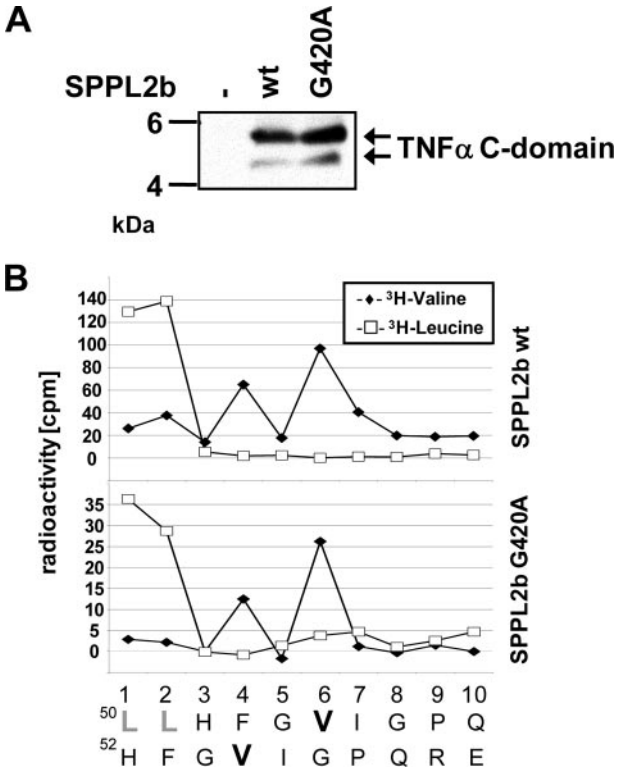


FIGURE 3. **The C-domain liberated from SPPL2b G420A-expressing cells is unchanged as compared with SPPL2b wt.** *A*, generation of the TNF$\alpha$ C-domain. Conditioned media of HEK 293 cells stably expressing the indicated SPPL2b variants and transiently expressing TNF$\alpha\Delta$E (12) were analyzed for the TNF$\alpha$ C-domain using antibodies against the HA tag. Note that the TNF$\alpha$ C-domain species secreted in cells expressing SPPL2b wt and in cells expressing SPPL2b G420A show identical running behavior. *B*, radiosequencing of the TNF$\alpha$ C-domain in SPPL2b G420A mutant cell lines. Cell lines described in *A* were labeled with either [$^3$H]valine (♦) or [$^3$H]leucine (□). Radiosequencing of the isolated TNF$\alpha$ C-domain reveals identical TNF$\alpha$ C-domain species in both cell lines starting at Leu-50 or His-52. Both C-domain species detected in *A* have the same N terminus and probably slightly differ in either their C terminus or their structure.

*Mutant SPPL2b Slows Sequential Intramembrane Proteolysis*—To investigate a putative stepwise conversion of TNF$\alpha$ into its ICD fragments as it has been suggested for $\gamma$-secretase cleavage of APP (22, 39–41) we performed *in vitro* processing experiments. Membranes of cells co-expressing wt SPPL2b or SPPL2b G420A and TNF$\alpha$ were incubated for various time points, and cleavage products were separated on Tris-Tricine gels. Surprisingly, this revealed that both wt and mutant SPPL2b variants initiate intramembrane proteolysis of TNF$\alpha$ with the production of a co-migrating peptide, designated ICD peptide 1 (Fig. 4*A*). At 1 h, ICD peptide 1 was rapidly processed by wt SPPL2b via an intermediate peptide (ICD peptide 2) to the fast migrating ICD peptide 3 (Fig. 4*A*). In contrast, ICD peptide 1 was significantly slower turned over by SPPL2b G420A. Only after 6 h of incubation, ICD peptide 1 was at least partially turned over to ICD peptide 2, but at this time point no ICD peptide 3 was observed (Fig. 4*A*). Moreover, the TNF$\alpha$ NTF, which represents the immediate substrate for SPPL2b, was rapidly turned

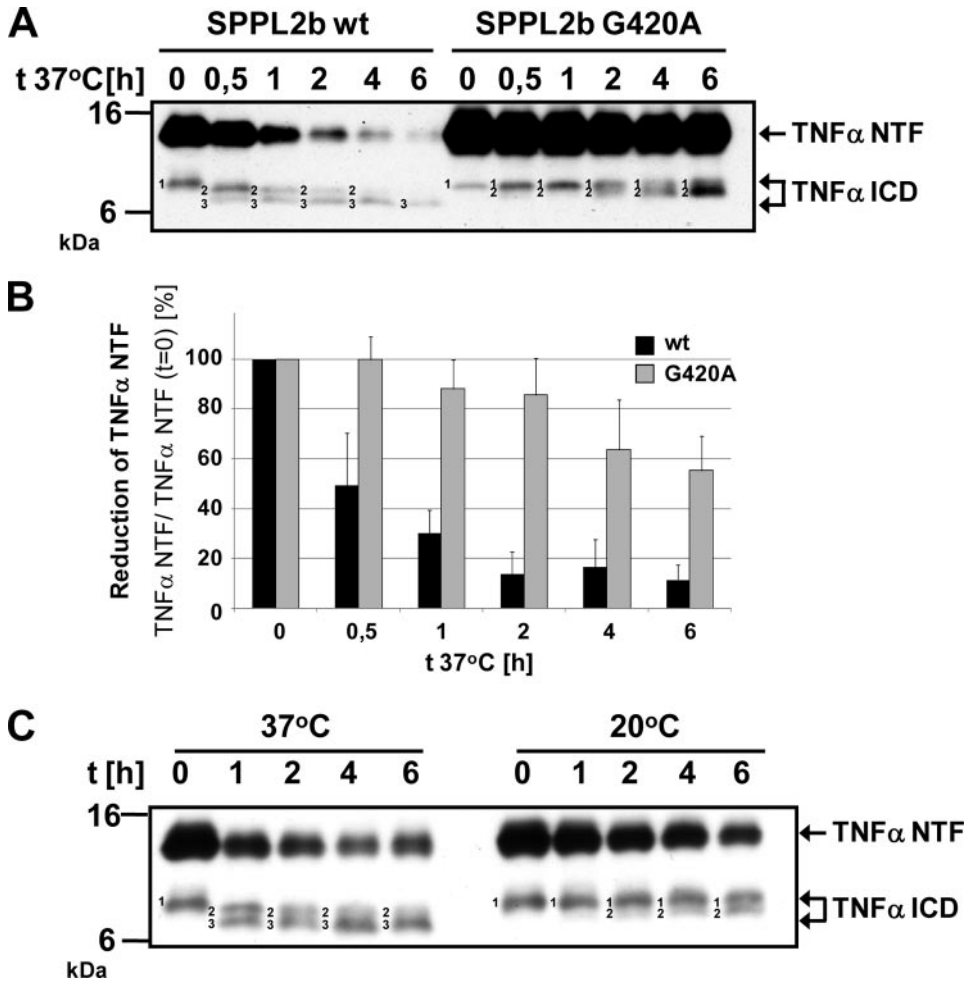


FIGURE 4. **Conversion of the TNFα ICD is slowed in cells expressing the SPPL2b G420A mutant.** *A*, time-dependent conversion of TNFα ICD. Cellular membranes of HEK 293 cells co-expressing the indicated SPPL2b variants and TNFα FL were isolated and incubated for the indicated time periods at 37 °C. TNFα ICD species were separated using a modified Tris-Tricine gel and were visualized using the anti-FLAG antibody. Three major TNFα ICD species are detectable (designated *1–3*). TNFα ICD 1 is converted over time to ICD 2 and finally to ICD 3. The conversion of TNFα ICD 1 over time is significantly slower in cells expressing SPPL2b G420A compared with cells expressing SPPL2b wt. Note the accumulation of TNFα ICD 2 in SPPL2b G420A-expressing cells. *B*, quantitative measurement of the TNFα NTF conversion. The signal intensity of TNFα NTF shown in *A* was measured at the indicated time points of incubation and determined in relation to the TNFα NTF signal at time point 0. Values represent means ± S.D. of three independent experiments. *C*, conversion of the TNFα ICD at reduced incubation temperature. TNFα ICD conversion in membranes expressing SPPL2b wt is significantly slower upon incubation at 20 °C as compared with incubation at 37 °C. Note the accumulation of TNFα ICD 2 upon incubation at 20 °C.

over by wt SPPL2b, whereas this fragment accumulated in cells expressing the G420A mutation (Fig. 4, *A* and *B*). Very similar findings were observed when independent cell clones were used (data not shown). This suggests that mutant SPPL2b is proteolytically active but may exhibit a reduced turnover rate. If that was the case one would expect that, upon prolonged incubation time periods, mutant SPPL2b should be capable of producing at least some ICD peptide 3. Indeed, upon 22 h of incubation, a peptide co-migrating with ICD peptide 3 was produced by cells expressing SPPL2b G420A at least to some extend (supplemental Fig. S1). Moreover, when membranes of cells co-expressing wt SPPL2b and TNFα were incubated at lower temperature to mimic reduced turnover, TNFα NTF also accumulated over time (Fig. 4*C*). Thus, if wt SPPL2b is incubated under suboptimal conditions, reduced processing of the TNFα NTF and the resulting TNFα ICD peptides leads to an altered ratio of long, intermediate, and short ICD peptides, such as those observed for the SPPL2b G420A mutation.

The above-described findings do not exclude the possibility that the ICD peptides 2 and 3 are produced by trimming proteases rather than SPPL2b. Clearly the initial cleavage is performed by SPPL2b, because $(Z\text{-}LL)_2$-ketone (see Fig. 2*E*) as well as expression of the functional inactive SPPL2b D421A mutation (16) (Fig. 5*A*) inhibits its formation. Moreover, co-incubation of membrane fractions with a broad-spectrum protease inhibitor mixture failed to significantly slow ICD turnover (Fig. 5*B*). To finally prove that SPPL2b is the major converting enzyme of all TNFα ICD species, we added $(Z\text{-}LL)_2$-ketone after 0.2 h of *in vitro* incubation to the membrane fractions and analyzed ICD generation at the indicated time points (Fig. 5*C*). Without addition of $(Z\text{-}LL)_2$-ketone, ICD peptide 2 continued to be turned over, whereas the addition of $(Z\text{-}LL)_2$-ketone blocks conversion of the TNFα ICD species (compare ratios of ICD species 2 and 3 in Fig. 5*C* at $t = 4$ h), demonstrating that all ICD peptides were generated by the intrinsic proteolytic activity of SPPL2b. Together with the data in Fig. 4 these findings therefore suggest a sequential processing of TNFα by SPPL2b. However, in contrast to wt SPPL2b, which rapidly produces the smaller ICD peptides, mutant SPPL2b G420A shows a significantly reduced turnover rate suggesting a partial loss of function.

*The FAD-associated PS1 G384A Selectively Slows Aβ40 Generation*—Similar *in vitro* experiments were then performed with partially purified γ-secretase derived from cells expressing PS1 wt or the PS1 G384A mutation. This revealed that γ-secretase containing the PS1 G384A mutation shows a slowed turnover of the recombinant APP substrate C100-$His_6$ *in vitro* as compared with wt PS1, because AICD generation and production of total Aβ were reduced (Fig. 6). However, comparison of the time-dependent production of Aβ40 and Aβ42 by wt or mutant γ-secretase revealed a selectively slowed Aβ40 production by γ-secretase containing the PS1 G384A mutation (Fig. 5). Thus, slower Aβ40 production by γ-secretase containing the G384A PS1 mutant leads to the change in the Aβ42 to Aβ40 ratio.

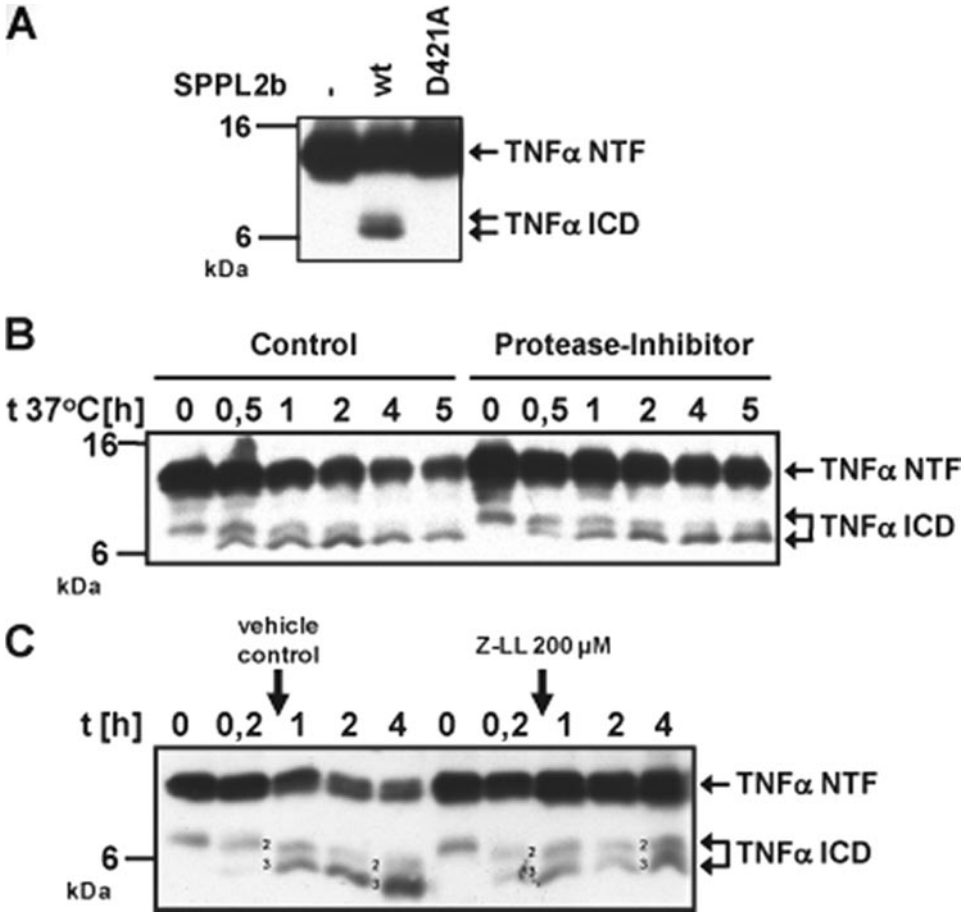


FIGURE 5. **TNF$\alpha$ ICD conversion is catalyzed by SPPL2b.** *A*, expression of SPPL2b D421A completely abolishes TNF$\alpha$ ICD production. Membranes of HEK 293 cells co-expressing TNF$\alpha$ FL and the indicated SPPL2b variants were incubated for 60 min at 37 °C, and ICD production was monitored as described in Fig. 2*D*. Note that expression of the proteolytically inactive SPPL2b D421A completely abolishes ICD production. *B*, conversion of the TNF$\alpha$ ICDs is not related to nonspecific proteases. Membranes of HEK 293 cells co-expressing TNF$\alpha$ FL and SPPL2b wt were treated with either protease inhibitor mixture or vehicle and incubated for the indicated time periods at 37 °C. Note that protease inhibitor treatment does not affect TNF$\alpha$ ICD conversion. *C*, $(Z\text{-}LL)_2$-ketone treatment stabilizes TNF$\alpha$ ICD intermediates. Membranes of HEK 293 cells co-expressing TNF$\alpha$ FL and SPPL2b wt were incubated for the indicated time periods at 37 °C. After 10-min incubation time 200 $\mu$M $(Z\text{-}LL)_2$-ketone or vehicle was added to the sample series. Note that after addition of $(Z\text{-}LL)_2$-ketone the turnover of TNF$\alpha$ ICD species is blocked, whereas it proceeds in vehicle control-treated samples.

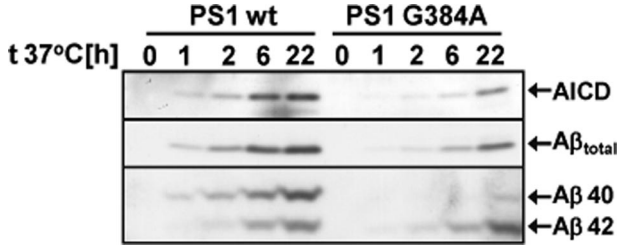


FIGURE 6. **Selective reduction of A$\beta$40 generation by PS1 G384A.** $\gamma$-Secretase complexes containing PS1 wt or PS1 G384A were isolated from HEK 293 cells and incubated with recombinant C100-$His_6$ at 37 °C for the indicated time periods. A$\beta$ peptides were separated as described (33) and detected using the anti-A$\beta$ antibody 6E10. Note that A$\beta$40 production is selectively slowed by $\gamma$-secretase containing PS1 G384A as compared with PS1 wt.

## DISCUSSION

Until recently intramembrane proteolysis was thought to be rather impossible, because water molecules, which are required for all proteolytic enzymes, are rare within the hydrophobic lipid bilayer of the membrane. However, a surprising number of intramembrane proteases have been identified during the last few years (1, 43). These include metalloproteases, such as site-2 proteases (44), serine proteases, such as the large family of rhomboids (43) and aspartyl proteases, including $\gamma$-secretase with PSs as catalytically active subunits (45, 46), type 4 prepilin peptidases (47), and SPP/SPPL family members (10, 16, 23). The latter are all defined by a critical G*X*GD active site motif (1, 8, 9, 16). Mutagenesis not only of the critical aspartate but also of the glycine residue immediately adjacent to the aspartate residue affects $\gamma$-secretase activity, by either blocking its activity or by modulating cleavage precision (9). Moreover, at least in PS1 the amino acid located at position *X* of the G*X*GD domain is involved in the final substrate selection at the active site (48). Beside the conserved G*X*GD and YD active site domains, PS and SPP/SPPL family members also share a conserved PAL motif, which is likely to interact with the catalytic center of G*X*GD-type proteases (37). Numerous FAD-associated mutations have been identified within PS1 and some within PS2 (46). All PS mutations occur at evolutionary conserved amino acids and apparently modulate the precision of $\gamma$-secretase cleavage. Although the pathological activity of PS mutations in terms of increasing the A$\beta$42:A$\beta$40 ratio has been known for a long time, the molecular mechanisms behind these consistent changes in proteolysis of APP are rather unclear today. So far some studies implicate a structural change of PS, because PS-associated FAD mutations seem to affect the distance between the N- and C-terminal fragments of PS (25). Others implicate a loss of function, because PS mutations fail to efficiently rescue a loss of the *C. elegans* homologue sel-12 (26, 27). Indeed at least the rather aggressive PS mutations exhibit reduced overall A$\beta$ production when expressed in a complete PS-free background (38). However, some PS1 mutations also fully rescue the developmental abnormalities of a PS1 knockout (29). To gain more insight into the mechanism of FAD-associated PS mutations and to understand intramembrane proteolysis by G*X*GD-type proteases, we introduced the PS1 G384A mutation at the corresponding position in SPPL2b. This mutation was specifically chosen because the corresponding glycine residue is fully conserved in all SPP/SPPL members (10, 11, 16), whereas PS mutations outside of the G*X*GD motif largely occur at positions that do not share sequence conservation with SPP/SPPL family members. Surprisingly, the introduction of this

mutation into SPPL2b resulted in a slowed turnover of TNFα NTF, and the resulting longer TNFα ICD species, whereas the cleavage site of the secreted TNFα C-domain was unaffected. Thus, our findings provide strong evidence for the hypothesis that the active site domains of SPP/SPPL family members are not only reversed in their orientation as compared with PS (23) but also act in a reversed manner. Consistent with the opposite orientation of all known substrates for SPP/SPPL family members (10, 12, 13, 15), our findings suggest that the TNFα ICD released into the cytosol topologically corresponds to the secreted Aβ-domain or similar peptides released from various substrates by γ-secretase. The secreted C-domain on the other hand may reflect an ϵ-like cleavage, which in the case of APP or Notch would liberate the cytoplasmic APP KD or Notch ICD (19–21).

Our *in vitro* experiments allowed for the first time a sensitive time resolution of intramembrane proteolysis. This revealed a stepwise sequential processing. Based on our findings longer ICD species are sequentially turned over to shorter ICD species. After an initiating ϵ-like cut, releasing the C-domain, further cleavages occur, which result in the generation of smaller fragments probably corresponding to a γ- and/or ζ-like cleavage of APP (22, 39, 40). Our findings suggest that the TNFα substrate may pass through a pore-like active site domain, or at least a hydrophilic cavity, step-by-step, moving along the protease active site, which itself remains locked at its original location. Such a step-by-step mechanism may occur during or be supported by unfolding of the α-helical conformation of the TM domain of the substrate and explain how one substrate molecule is cleaved multiple times by one and the same membrane-embedded protease.

The *in vitro* experiments further demonstrated that cleavages by wt or mutant SPPL2b were qualitatively similar if not identical. These findings are therefore consistent with those obtained with a mutant SPP variant (18). However, the apparent accumulation of an elongated TNFα ICD turned out to be due to a reduced turnover rate of the mutant SPPL2b rather than a change in cleavage specificity. This further explains why for example after a 1-h incubation period SPPL2b G420A produces apparently longer ICD species than SPPL2b wt (see Fig. 2*D*). Extensive incubation times allowed mutant SPPL2b to finally generate at least some ICDs, which were similar to those produced by wt SPPL2b. Therefore, the FAD-like mutation of SPPL2b surprisingly confers neither a full loss nor a gain of function but, rather, reduces substrate turnover. This could be mimicked when wt SPPL2b was incubated at low temperature. Under these conditions reduced turnover also caused a relative increase of larger ICD fragments over the shorter versions such as those seen in SPPL2b G420A-expressing cells.

Similar findings were made for γ-secretase containing the G384A mutant PS1. In that case, however, Aβ40 generation was selectively slowed by mutant γ-secretase as compared with wt. Although Aβ40 was still detectable, its production was significantly reduced, and much longer incubation times were needed to generate detectable levels of Aβ40 (compare time point 6 h in Fig. 6). Similar findings were recently described for the PS1 I213T mutation, which also selectively affects Aβ40 generation (49). Due to its rather aggressive behavior, strongly altered cleavage specificity is observed for G384A with Aβ42 considerably exceeding the amount of Aβ40. However, no apparent precursor-product relationship between Aβ42 and Aβ40 was observed in the time-course analysis suggesting that these peptides might be derived from two independent product lines consistent with the model suggested by Qi-Takahara and colleagues (22). This model implies two independent cleavage events at the ϵ-cleavage site (at positions 49 and 48 of the Aβ domain) initiating two independent product lines. The initial cut at position 49 is predicted to result in a trimming event producing Aβ46, Aβ43, and Aβ40, whereas the cut at position 48 results in products terminating at positions 45, 42, and 39. Our findings suggest that the product line leading to Aβ40 is selectively slowed at least by an aggressive PS mutation, whereas the Aβ42-generating product line is unaffected or may even be increased. Selective reduction of Aβ40 generation as a cellular mechanism of FAD-associated PS mutations is also consistent with recent findings demonstrating that Aβ40 interferes with Aβ42 deposition in transgenic mice probably by inhibiting its aggregation (50). Conformational interference with Aβ aggregation is also supported by the recent finding that overexpression of cystatin C reduces Aβ deposition (51). Thus one may predict that FAD-associated PS mutations selectively reduce the generation of an anti-amyloidogenic Aβ species, and thus accelerate Aβ42 aggregation. Clearly, other PS mutations in addition to the PS1 G384A and I213T must be investigated to further support this hypothesis. We have recently investigated the PS1 L166P mutation and again found slowed Aβ40 production[5] as a cause for the change in the Aβ42/Aβ40 ratio. However, one should keep in mind that not all FAD-associated PS mutations must result in a loss of Aβ40 production. Week mutations with a fairly late age of onset may show other mechanisms (and thus rescue a PS knockout phenotype; see above) or the effects on Aβ40 reduction may be too subtle to be investigated. Here we specifically investigated the very aggressive PS1 G384A mutation, because it occurs at a position that is fully conserved in all members of the SPP/SPPL and PS family.

Our findings also have implications for the use of γ-secretase as a therapeutic target. Multiple reports demonstrated that robust inhibition of γ-secretase *in vivo* results in rather severe side-effects due to the inhibition of the physiological function of γ-secretase in Notch signaling (42, 52). Therefore, a window allowing sufficient activity of γ-secretase for its physiological function while reducing γ-secretase activity significantly enough to slow Aβ production needs to be defined. At too low concentrations of γ-secretase inhibitors as well as upon termination of γ-secretase treatment in patients, increased Aβ42 production may occur. This is indeed the case in patients treated with γ-secretase inhibitors and in cells grown in the presence of a low dose of certain γ-secretase inhibitors (for review see Ref. 32). Thus such a window may be much narrower than expected, and dosing of γ-secretase inhibitors needs to be extremely carefully monitored to prevent opposite effects.

[5] H. Steiner and C. Haass, submitted for publication.

## REFERENCES


1. Weihofen, A., and Martoglio, B. (2003) *Trends Cell Biol.* **13,** 71–78
2. Shoji, M., Golde, T. E., Ghiso, J., Cheung, T. T., Estus, S., Shaffer, L. M., Cai, X. D., McKay, D. M., Tintner, R., Frangione, B., and Younkin, S. (1992) *Science* **258,** 126–129
3. Haass, C., Schlossmacher, M. G., Hung, A. Y., Vigo-Pelfrey, C., Mellon, A., Ostaszewski, B. L., Lieberburg, I., Koo, E. H., Schenk, D., Teplow, D. B., and Selkoe, D. J. (1992) *Nature* **359,** 322–325
4. Busciglio, J., Gabuzda, D. H., Matsudaira, P., and Yankner, B. A. (1993) *Proc. Natl. Acad. Sci. U. S. A.* **90,** 2092–2096
5. Kopan, R., and Ilagan, M. X. (2004) *Nat. Rev. Mol. Cell. Biol.* **5,** 499–504
6. Haass, C. (2004) *EMBO J.* **23,** 483–488
7. Edbauer, D., Winkler, E., Regula, J. T., Pesold, B., Steiner, H., and Haass, C. (2003) *Nat. Cell Biol.* **5,** 486–488
8. Haass, C., and Steiner, H. (2002) *Trends Cell Biol.* **12,** 556–562
9. Steiner, H., Kostka, M., Romig, H., Basset, G., Pesold, B., Hardy, J., Capell, A., Meyn, L., Grim, M. G., Baumeister, R., Fechteler, K., and Haass, C. (2000) *Nat. Cell Biol.* **2,** 848–851
10. Weihofen, A., Binns, K., Lemberg, M. K., Ashman, K., and Martoglio, B. (2002) *Science* **296,** 2215–2218
11. Ponting, C. P., Hutton, M., Nyborg, A., Baker, M., Jansen, K., and Golde, T. E. (2002) *Hum. Mol. Genet.* **11,** 1037–1044
12. Fluhrer, R., Grammer, G., Israel, L., Condron, M. M., Haffner, C., Friedmann, E., Bohland, C., Imhof, A., Martoglio, B., Teplow, D. B., and Haass, C. (2006) *Nat. Cell Biol.* **8,** 894–896
13. Kirkin, V., Cahuzac, N., Guardiola-Serrano, F., Huault, S., Luckerath, K., Friedmann, E., Novac, N., Wels, W. S., Martoglio, B., Hueber, A. O., and Zornig, M. (2007) *Cell Death Differ.* **14,** 1678–1687
14. Friedmann, E., Hauben, E., Maylandt, K., Schleeger, S., Vreugde, S., Lichtenthaler, S. F., Kuhn, P. H., Stauffer, D., Rovelli, G., and Martoglio, B. (2006) *Nat. Cell Biol.* **8,** 843–848
15. Martin, L., Fluhrer, R., Reiss, K., Kremmer, E., Saftig, P., and Haass, C. (2008) *J. Biol. Chem.* **283,** 1644–1652
16. Krawitz, P., Haffner, C., Fluhrer, R., Steiner, H., Schmid, B., and Haass, C. (2005) *J. Biol. Chem.* **280,** 39515–39523
17. Loureiro, J., Lilley, B. N., Spooner, E., Noriega, V., Tortorella, D., and Ploegh, H. L. (2006) *Nature* **441,** 894–897
18. Sato, T., Nyborg, A. C., Iwata, N., Diehl, T. S., Saido, T. C., Golde, T. E., and Wolfe, M. S. (2006) *Biochemistry* **45,** 8649–8656
19. Weidemann, A., Eggert, S., Reinhard, F. B., Vogel, M., Paliga, K., Baier, G., Masters, C. L., Beyreuther, K., and Evin, G. (2002) *Biochemistry* **41,** 2825–2835
20. Sastre, M., Steiner, H., Fuchs, K., Capell, A., Multhaup, G., Condron, M. M., Teplow, D. B., and Haass, C. (2001) *EMBO Rep.* **2,** 835–841
21. Gu, Y., Misonou, H., Sato, T., Dohmae, N., Takio, K., and Ihara, Y. (2001) *J. Biol. Chem.* **276,** 35235–35238
22. Qi-Takahara, Y., Morishima-Kawashima, M., Tanimura, Y., Dolios, G., Hirotani, N., Horikoshi, Y., Kametani, F., Maeda, M., Saido, T. C., Wang, R., and Ihara, Y. (2005) *J. Neurosci.* **25,** 436–445
23. Friedmann, E., Lemberg, M. K., Weihofen, A., Dev, K. K., Dengler, U., Rovelli, G., and Martoglio, B. (2004) *J. Biol. Chem.* **279,** 50790–50798
24. Haass, C., and Selkoe, D. J. (2007) *Nat. Rev. Mol. Cell. Biol.* **8,** 101–112
25. Berezovska, O., Lleo, A., Herl, L. D., Frosch, M. P., Stern, E. A., Bacskai, B. J., and Hyman, B. T. (2005) *J. Neurosci.* **25,** 3009–3017
26. Levitan, D., Doyle, T. G., Brousseau, D., Lee, M. K., Thinakaran, G., Slunt, H. H., Sisodia, S. S., and Greenwald, I. (1996) *Proc. Natl. Acad. Sci. U. S. A.* **93,** 14940–14944
27. Baumeister, R., Leimer, U., Zweckbronner, I., Jakubek, C., Grunberg, J., and Haass, C. (1997) *Genes Funct.* **1,** 149–159
28. Moehlmann, T., Winkler, E., Xia, X., Edbauer, D., Murrell, J., Capell, A., Kaether, C., Zheng, H., Ghetti, B., Haass, C., and Steiner, H. (2002) *Proc. Natl. Acad. Sci. U. S. A.* **99,** 8025–8030
29. Davis, J. A., Naruse, S., Chen, H., Eckman, C., Younkin, S., Price, D. L., Borchelt, D. R., Sisodia, S. S., and Wong, P. C. (1998) *Neuron* **20,** 603–609
30. De Strooper, B. (2007) *EMBO Rep.* **8,** 141–146
31. Wolfe, M. S. (2007) *EMBO Rep.* **8,** 136–140
32. Shen, J., and Kelleher, R. J., 3rd (2007) *Proc. Natl. Acad. Sci. U. S. A.* **104,** 403–409
33. Wiltfang, J., Smirnov, A., Schnierstein, B., Kelemen, G., Matthies, U., Klafki, H. W., Staufenbiel, M., Huther, G., Ruther, E., and Kornhuber, J. (1997) *Electrophoresis* **18,** 527–532
34. Weihofen, A., Lemberg, M. K., Ploegh, H. L., Bogyo, M., and Martoglio, B. (2000) *J. Biol. Chem.* **275,** 30951–30956
35. Fluhrer, R., Capell, A., Westmeyer, G., Willem, M., Hartung, B., Condron, M. M., Teplow, D. B., Haass, C., and Walter, J. (2002) *J. Neurochem.* **81,** 1011–1020
36. Fluhrer, R., and Haass, C. (2007) *Neurodegener. Dis.* **4,** 112–116
37. Wang, J., Beher, D., Nyborg, A. C., Shearman, M. S., Golde, T. E., and Goate, A. (2006) *J. Neurochem.* **96,** 218–227
38. Bentahir, M., Nyabi, O., Verhamme, J., Tolia, A., Horre, K., Wiltfang, J., Esselmann, H., and De Strooper, B. (2006) *J. Neurochem.* **96,** 732–742
39. Zhao, G., Cui, M. Z., Mao, G., Dong, Y., Tan, J., Sun, L., and Xu, X. (2005) *J. Biol. Chem.* **280,** 37689–37697
40. Zhao, G., Mao, G., Tan, J., Dong, Y., Cui, M. Z., Kim, S. H., and Xu, X. (2004) *J. Biol. Chem.* **279,** 50647–50650
41. Sato, T., Dohmae, N., Qi, Y., Kakuda, N., Misonou, H., Mitsumori, R., Maruyama, H., Koo, E. H., Haass, C., Takio, K., Morishima-Kawashima, M., Ishiura, S., and Ihara, Y. (2003) *J. Biol. Chem.* **278,** 24294–24301
42. Geling, A., Steiner, H., Willem, M., Bally-Cuif, L., and Haass, C. (2002) *EMBO Rep.* **3,** 688–694
43. Lemberg, M. K., and Freeman, M. (2007) *Mol. Cell* **28,** 930–940
44. Rawson, R. B., Zelenski, N. G., Nijhawan, D., Ye, J., Sakai, J., Hasan, M. T., Chang, T. Y., Brown, M. S., and Goldstein, J. L. (1997) *Mol. Cell* **1,** 47–57
45. Wolfe, M. S., Xia, W., Ostaszewski, B. L., Diehl, T. S., Kimberly, W. T., and Selkoe, D. J. (1999) *Nature* **398,** 513–517
46. Selkoe, D. J., and Wolfe, M. S. (2007) *Cell* **131,** 215–221
47. LaPointe, C. F., and Taylor, R. K. (2000) *J. Biol. Chem.* **275,** 1502–1510
48. Yamasaki, A., Eimer, S., Okochi, M., Smialowska, A., Kaether, C., Baumeister, R., Haass, C., and Steiner, H. (2006) *J. Neurosci.* **26,** 3821–3828
49. Shimojo, M., Sahara, N., Mizoroki, T., Funamoto, S., Morishima-Kawashima, M., Kudo, T., Takeda, M., Ihara, Y., Ichinose, H., and Takashima, A. (2008) *J. Biol. Chem.* **283,** 16488–16496
50. Kim, J., Onstead, L., Randle, S., Price, R., Smithson, L., Zwizinski, C., Dickson, D. W., Golde, T., and McGowan, E. (2007) *J. Neurosci.* **27,** 627–633
51. Kaeser, S. A., Herzig, M. C., Coomaraswamy, J., Kilger, E., Selenica, M. L., Winkler, D. T., Staufenbiel, M., Levy, E., Grubb, A., and Jucker, M. (2007) *Nat. Genet.* **39,** 1437–1439
52. Doerfler, P., Shearman, M. S., and Perlmutter, R. M. (2001) *Proc. Natl. Acad. Sci. U. S. A.* **98,** 9312–9317